A self-consistent extension of flamelet theory for partially premixed combustion

Hernan Olguin, Pascale Domingo, Luc Vervisch, Christian Hasse, Arne Scholtissek

A self-consistent extension of flamelet theory for partially premixed combustion

Hernan Olguin[a,*], Pascale Domingo[b], Luc Vervisch[b], Christian Hasse[c], Arne Scholtissek[c,**]

[a] *Department of Mechanical Engineering, Universidad Técnica Federico Santa María, Avenida España 1680, Valparaíso, Chile;*
[b] *CORIA CNRS, Normandie Université, INSA de Rouen, Technopôle du Madrillet, BP 8, Saint-Etienne-du-Rouvray 76801, France;*
[c] *Institute for Simulation of Reactive Thermo-Fluid Systems, TU Darmstadt, Otto-Berndt-Straße 2, 64287 Darmstadt, Germany;*

Abstract

Orthogonal coordinate systems represent an attractive alternative for the formulation of two-dimensional composition space equations for partially premixed combustion: They avoid the need of closure models for a cross scalar dissipation rate and allow for a direct recovery of the corresponding flamelet equations in the asymptotic limits of non-premixed and premixed combustion. Despite these remarkable features, this kind of coordinate systems still present some important unsolved issues, which have limited their application so far. These difficulties are mainly associated with i) the lack of an appropriate formalism for the definition of two variables having orthogonal gradients in the entire flame domain and ii) the absence of corresponding closure models for the gradients of these variables in two-dimensional composition space. In the present work, it is shown how a Lagrangian interpretation of the flamelet derivative allows solving both problems. More specifically, after the mixture fraction, Z, is adopted as first coordinate, the proposed approach allows to derive i) two-dimensional composition space equations for all reactive scalars, ii) a transport equation for a modified reaction progress variable, φ, satisfying the desired orthogonality condition, $\nabla Z \cdot \nabla \varphi = 0$, and iii) two-dimensional composition space equations for $g_Z = |\nabla Z|$ and $g_\varphi = |\nabla \varphi|$. The obtained set of two-dimensional equations in orthogonal composition space is general and it can describe different flames of interest. In order to illustrate the capabilities of the formulation, the equations are then specialized for planar flames with unity Lewis number, obtaining in this way a solvable set of composition space equations in orthogonal coordinates. After an appropriate numerical approach is introduced, the resulting 2D equations are solved to analyze the interaction between premixed flamelets with a strain rate prescribed along the Z-dimension controlling the interaction. Both

*Corresponding author
**Corresponding author
Email addresses: hernan.olguin@usm.cl (Hernan Olguin), scholtissek@stfs.tu-darmstadt.de (Arne Scholtissek)

flame structures and budgets of the scalar gradient equations are studied and the results provide new insights into the physics of scalar gradients in two-dimensional composition space. Finally, conceivable coupling strategies of the present formulation with CFD codes for the simulation of turbulent flames are discussed.

Keywords: Flamelet theory; Partially premixed combustion; Scalar gradient equations; Orthogonal composition space

1. Introduction

During the last decades, several sets of flamelet equations (also called one-dimensional composition space equations) have been derived and analyzed for non-premixed [1–4], premixed [5–9] and spray flames [10–14]. While these formulations work very well in the corresponding asymptotic limit for which they were developed, it is well known that they are not appropriate for more complex flames likely to be found in advanced combustion systems. Of particular interest are partially premixed flames (also called multi-regime flames), in which premixed and non-premixed combustion modes can co-exist and interact [15, 16]. Therefore, several different sets of two-dimensional composition space equations have been proposed in recent years as extensions of the classical flamelet theory [17–22], all of which make use of the mixture fraction, Z, and a second conditioning variable, generalized here as φ, to define the composition space, (Z, φ, τ), where τ is a time-like variable. Typically, φ is defined as some sort of reaction progress variable [17–23], but approaches using a second mixture fraction [24] or enthalpy [25] also exist. For a comprehensive review of the associated literature on two-dimensional composition space equations, the reader is referred to the recent works of Mueller and coworkers [21, 23] and Scholtissek et al. [22].

While the use of non-orthogonal coordinates represents the most common choice for the formulation of two-dimensional composition space equations, Scholtissek et al. [22] have recently shown how an orthogonal coordinate system can be defined based on the mixture fraction and a conventional reaction progress variable, Y_c. In particular, they introduced the following transformation rule from physical into composition space

$$\nabla(\cdot) = \frac{\partial(\cdot)}{\partial Z}\nabla Z + \left.\frac{\partial(\cdot)}{\partial Y_c}\right|_Z \nabla_\perp Y_c, \tag{1}$$

where $|_Z$ indicates that a derivative has been taken keeping Z constant and

$$\nabla_\perp Y_c = \nabla Y_c - (\mathbf{n}_Z \cdot \nabla Y_c)\mathbf{n}_Z \tag{2}$$

is defined as the component of ∇Y_c perpendicular to ∇Z, with $\mathbf{n}_Z = \nabla Z/|\nabla Z|$ denoting an unit vector normal to the Z-isosurfaces. Based on this transformation, a set of composition space

equations for chemical species and temperature was then derived and validated in the context of triple flame structures obtained by means of numerical simulations [22].

One of the major advantages associated with the use of orthogonal composition space coordinates is avoiding the need of closure models for the cross scalar dissipation rate, $\chi_{Z\varphi} = 2D\ \nabla Z \cdot \nabla\varphi$, since this quantity is identically zero by construction. This directly solves one of the most important problems related with the development of a general two-dimensional composition space theory in non-orthogonal coordinates, making the approach of Scholtissek et al. [22] very attractive. Additionally, Eq. (1) conveniently reduces in the asymptotic limits of non-premixed and premixed combustion, which allows a direct and transparent recovery of the respective classical flamelet equations in those situations. More specifically, for non-premixed flames the gradients of Z and Y_c tend to align, which implies that $\nabla_\perp Y_c \to 0$ (the component of ∇Y_c perpendicular to ∇Z vanishes). This reduces Eq. (1) to $\nabla(\cdot) \approx \partial(\cdot)/\partial Z\ \nabla Z$, which corresponds to the classical flamelet transformation for non-premixed flames [1, 15]. For the limit of premixed combustion, on the other hand, $\nabla Z \to 0$, which implies that $\nabla_\perp Y_c \to \nabla Y_c$, since $\mathbf{n}_Z \cdot \nabla Y_c = |\nabla Z|\partial Y_c/\partial Z \approx 0$ in this limit (see Eq. (2)). Accordingly, for this case Eq. (1) reduces to $\nabla(\cdot) \approx \partial(\cdot)/\partial Y_c\ \nabla Y_c$, which coincides with the transformation rules used in previous works in the context of one-dimensional premixed flamelets [26, 9]. Due to all these positive features, the use of orthogonal coordinates in composition space results very promising, motivating new research efforts on the topic.

However, while conceptually very powerful, the approach introduced by Scholtissek et al. [22] still presents some open issues, which have limited its application so far. First, an explicit definition for the second coordinate, φ, ensuring a gradient of this quantity perpendicular to ∇Z in the flame zone has not yet been provided. Instead, as illustrated in Eq. (1), the authors employed partial derivatives with respect to Y_c while keeping Z constant to express all terms in the equations as a function of Z, Y_c and τ only. While at a first glance this may appear as an unimportant detail, it can be very restrictive in practice. In particular, computing $\partial(\cdot)/\partial Y_c|_Z$ and $\nabla_\perp Y_c$ requires a priori knowledge of the angle between ∇Z and ∇Y_c, which is equivalent to knowing the cross scalar dissipation rate. Additionally, the absence of an explicit equation for φ hinders the derivation of appropriate closure models for the conditioning scalar gradients, $g_Z = |\nabla Z|$ and $g_\varphi = |\nabla\varphi|$, which are required for the development of a solvable set of composition space equations.

The **major objective** of the present work is addressing the open issues of the formulation of Scholtissek et al. [22], while keeping its important advantages. More specifically, we aim to develop a self-consistent composition space theory for partially premixed flames in orthogonal coordinates (Z, φ, τ), including the following main components:

C_1: A simple and general formalism for the derivation of two-dimensional composition space equations based on a Lagrangian interpretation of the temporal flamelet derivative, $\partial(\cdot)/\partial\tau|_{Z,\varphi}$, and a demonstration of its use in terms of the generic reactive scalar, ψ.

C_2: An extension of the formalism to obtain a transport equation for the second coordinate, φ, satisfying the required condition that $\nabla Z \cdot \nabla\varphi = 0$ in the flame region.

C_3: Further application of the proposed Lagrangian approach to obtain additional two-dimensional equations for g_Z and g_φ.

C_4: A specific formulation for unity Lewis number (without loss of generality) as an example of how a solvable set of equations can be obtained in terms of four parameters: the two strain rates, $a_Z = \mathbf{n}_Z \cdot \partial\mathbf{u}/\partial n_Z$ and $a_\varphi = \mathbf{n}_\varphi \cdot \partial\mathbf{u}/\partial n_\varphi$, with $\partial(\cdot)/\partial n$ denoting a directional derivative, and the two curvatures, $\kappa_Z = -\nabla \cdot \mathbf{n}_Z$ and $\kappa_\varphi = -\nabla \cdot \mathbf{n}_\varphi$, where $\mathbf{n}_\varphi = \nabla\varphi/|\nabla\varphi|$.

C_5: A demonstration of how the derived equations can be used to study the interaction between different combustion regimes together with a corresponding appropriate numerical approach for their solution.

Additionally, conceivable coupling strategies of the present formulation with CFD codes for the simulation of turbulent flames are discussed. This work is expected to provide an appropriate framework for a deep understanding of combustion physics in two-dimensional composition space, as well as a proper basis for future applications of the theory to the development of modelling strategies for the simulation of multi-regime turbulent flames.

2. General composition space formulation

In this section, the components C_1 (Section 2.1), C_2 (Section 2.2) and C_3 (Section 2.3) of the aimed two-dimensional composition space theory are developed. This is done in a general way, so that the approach can be easily specialized later for any particular case of interest.

2.1. Equation for a generic reactive scalar ψ

We start considering two variables, Z and φ, which are governed by

$$\frac{\partial Z}{\partial t} + \mathbf{u} \cdot \nabla Z = \Gamma_Z \tag{3}$$

and

$$\frac{\partial \varphi}{\partial t} + \mathbf{u} \cdot \nabla \varphi = \Gamma_\varphi, \tag{4}$$

respectively. Here, $\mathbf{u}$ is the flow velocity, and the right hand sides (RHSs) of the above equations, Γ_Z and Γ_φ, can contain diffusion, chemical reactions and even evaporation effects, depending on the considered flame type. While Z and φ will typically be a mixture fraction and some sort of reaction progress variable, respectively, there is no need of specifying Γ_Z and Γ_φ at this point and we will keep them general for now. Two unit vectors perpendicular to the Z and φ isosurfaces can be defined as

$$\mathbf{n}_Z = \frac{\nabla Z}{|\nabla Z|} \quad \text{and} \quad \mathbf{n}_\varphi = \frac{\nabla \varphi}{|\nabla \varphi|}, \tag{5}$$

respectively. Since we aim to work on an orthogonal coordinate system, it will be imposed now that $\mathbf{n}_Z \cdot \mathbf{n}_\varphi = 0$, and this condition, together with other requirements identified later, will allow determining an explicit form for Γ_φ.

We introduce now the general reactive scalar, ψ, which is governed by the following equation

$$\frac{\partial \psi}{\partial t} + \mathbf{u} \cdot \nabla \psi = \Gamma_\psi, \tag{6}$$

where the transported variable could be the chemical species mass fraction, Y_k, or the temperature, T. We highlight at this point that a change of coordinates from $(\mathbf{x}, t)$ into (Z, φ, τ) could be directly utilized now to obtain a ψ composition space equation, as it is commonly done in the literature (see for example [17–22]). However, instead of that, we consider an alternative path here, for which we introduce a mass-less particle moving with velocity $\mathbf{u}_p$ given by

$$\mathbf{u}_p = \mathbf{u} - \frac{\Gamma_Z}{|\nabla Z|}\mathbf{n}_Z - \frac{\Gamma_\varphi}{|\nabla \varphi|}\mathbf{n}_\varphi. \tag{7}$$

Considering Eq. (7), it is easy to prove that this particle velocity simultaneously satisfies the kinematic conditions

$$\frac{\partial Z}{\partial t} + \mathbf{u}_p \cdot \nabla Z = 0 \quad \text{and} \quad \frac{\partial \varphi}{\partial t} + \mathbf{u}_p \cdot \nabla \varphi = 0, \tag{8}$$

which implies that the particle follows a point located at the intersection between a Z and a φ-isosurface. In other words, $\mathbf{u}_p$ is an extension of the classical definition of absolute velocity of a single scalar isosurface, which is composed of the flow velocity and the relative velocity of the iso-scalar surface (with respect to the flow) due to diffusion and reaction (see for example [27]). Now, since the temporal derivative in composition space can be interpreted as a Lagrangian derivative computed following the flame attached reference frame [28, 22], in the two-dimensional case considered here $\partial(\cdot)/\partial\tau|_{Z,\varphi}$ can be written as

$$\frac{\partial \psi}{\partial \tau} = \frac{\partial \psi}{\partial t} + \mathbf{u}_p \cdot \nabla \psi. \tag{9}$$

Making use of Eqs. (6) and (7), we can rewrite Eq. (9) as

$$\frac{\partial \psi}{\partial \tau} = \Gamma_\psi - \frac{\Gamma_Z}{|\nabla Z|}\frac{\partial \psi}{\partial n_Z} - \frac{\Gamma_\varphi}{|\nabla \varphi|}\frac{\partial \psi}{\partial n_\varphi}, \tag{10}$$

where $\partial(\cdot)/\partial n_\phi = \mathbf{n}_\phi \cdot \nabla(\cdot)$ is a directional derivative. With this procedure, the transformation of the temporal derivative through the application of the chain rule is avoided, which significantly reduces the effort involved in the derivation of the composition space equations. Introducing now the classical two-dimensional transformation rules for the spatial derivatives in physical space

$$\nabla \psi = \frac{\partial \psi}{\partial Z}\nabla Z + \frac{\partial \psi}{\partial \varphi}\nabla \varphi, \tag{11}$$

where the directional derivatives can be calculated as

$$\frac{\partial \psi}{\partial n_Z} = |\nabla Z|\frac{\partial \psi}{\partial Z} \quad \text{and} \quad \frac{\partial \psi}{\partial n_\varphi} = |\nabla \varphi|\frac{\partial \psi}{\partial \varphi}, \tag{12}$$

we can rewrite Eq. (10) as

$$\frac{\partial \psi}{\partial \tau} = \Gamma_\psi - \Gamma_Z\frac{\partial \psi}{\partial Z} - \Gamma_\varphi\frac{\partial \psi}{\partial \varphi}, \tag{13}$$

which describes the evolution of ψ on a flame attached reference frame simultaneously following isosurfaces of Z and φ.

The importance of both the procedure and the generalized composition space equation for ψ introduced in this section can be summarized now in two different aspects: First, even when a flamelet-type transformation, Eq. (11), is still required in the present derivation, introducing Eq. (9) leads to a procedure much simpler than the classical one, eliminating the need of transforming the temporal derivative and appropriately collecting terms. Secondly, given its quite remarkable generality, Eq. (13) represents a perfect starting point for the derivation of any particular specialized formulation in two-dimensional composition space. More specifically, Γ_ψ, Γ_Z and Γ_φ can be defined now with any degree of detail (including different effects such as differential diffusion, chemical reaction source terms, evaporation source terms and any other additional effect that could be required in any given case). After this, these terms just need to be transformed according to Eq. (11) and inserted in Eq. (13) directly, completely eliminating the need of repeating the above-presented derivation. This last aspect will be illustrated in the next section for the special case of unity Lewis number for all species (without loss of generality).

The formalism presented in this section corresponds to the component C_1 of the aimed composition space theory.

2.2. The φ-equation

We proceed now to obtain a general transport equation for φ, which requires specifying Γ_φ in terms of some already defined quantities. For this, two additional conditions are introduced here.

First, we will impose $\nabla\varphi = \nabla_\perp Y_c$, which will allow retaining all the advantage associated with the formulation by Scholtissek et al. [22] (see discussion in the introduction). After multiplying Eq. (2) by $\mathbf{n}_\varphi$ (dot product) and conveniently re-arranging, this first condition leads to

$$|\nabla\varphi|\frac{\partial Y_c}{\partial\varphi} = |\nabla\varphi|, \tag{14}$$

which can only be satisfied if

$$\frac{\partial Y_c}{\partial\varphi} = 1. \tag{15}$$

Before imposing the required second condition, we remark that, as defined in the previous subsection, the velocity $\mathbf{u}_p$ ensures by construction that a particle attached to a Z-isosurface remains on it when time advances. However, if all the characteristics of the premixed limit are to be recovered from the present formulation, we additionally need to ensure that the particle also remains attached to a corresponding Y_c-isosurface. For this, we consider the apparent flame velocity typically introduced in the context of premixed flames as

$$\mathbf{s}_f = \mathbf{u} - s_d\mathbf{n}_c, \tag{16}$$

with s_d denoting the flame displacement speed and where $\mathbf{n}_c = \nabla Y_c/|\nabla Y_c|$ corresponds to an unit vector normal to a reaction progress variable isosurface. With this apparent flame velocity, we can impose the condition

$$\mathbf{u}_p \cdot \mathbf{n}_c = \mathbf{s}_f \cdot \mathbf{n}_c, \tag{17}$$

which formally ensures that our mass-less particles will remain on the corresponding Y_c-isosurfaces as required.

We introduce now the following general governing equation for the reaction progress variable

$$\frac{\partial Y_c}{\partial t} + \mathbf{u}\cdot\nabla Y_c = \Gamma_c, \tag{18}$$

for which an extension of the analysis performed by Gibson [27] allows finding a explicit expression for s_d [15]. This yields

$$s_d = \frac{\Gamma_c}{|\nabla Y_c|}. \tag{19}$$

Using Eqs. (7), (19) and (17), we obtain

$$\Gamma_\varphi = \frac{|\nabla\varphi|}{(\mathbf{n}_\varphi\cdot\mathbf{n}_c)}\left[\frac{\Gamma_c}{|\nabla Y_c|} - \frac{\Gamma_Z}{|\nabla Z|}(\mathbf{n}_Z\cdot\mathbf{n}_c)\right], \tag{20}$$

which specifies Γ_φ as a function of Γ_c, Γ_Z and the scalar products between the different unit vectors associated with the scalar surfaces under consideration. The latter can be computed now as

$$\mathbf{n}_Z\cdot\mathbf{n}_c = \frac{|\nabla Z|}{|\nabla Y_c|}\frac{\partial Y_c}{\partial Z} \tag{21}$$

and

$$\mathbf{n}_\varphi \cdot \mathbf{n}_c = \frac{|\nabla\varphi|}{|\nabla Y_c|}, \tag{22}$$

respectively. With this, Eq. (20) reduces to

$$\Gamma_\varphi = \Gamma_c - \Gamma_Z \frac{\partial Y_c}{\partial Z}, \tag{23}$$

which can be inserted in Eq. (4) to obtain

$$\frac{\partial\varphi}{\partial t} + \mathbf{u}\cdot\nabla\varphi = \Gamma_c - \Gamma_Z \frac{\partial Y_c}{\partial Z}. \tag{24}$$

With this equation, the component C_2 of the aimed composition space theory has been specified.

2.3. Closure for the conditioning scalar gradients

While g_Z and g_φ do not explicitly appear in Eq. (13), it is well known that specifying Γ_ψ and applying the transformation rule given by Eq. (11) will lead to terms containing them. In order to close these quantities, we start considering a generic scalar, S, which obeys the following equation

$$\frac{\partial S}{\partial t} + \mathbf{u}\cdot\nabla S = \Gamma_S. \tag{25}$$

Since Eq. (25) has the same general form than Eqs. (3) and (4), we proceed now to derive a single equation for $g_S = |\nabla S|$, which can be then specialized for Z and φ.

To obtain a starting equation in physical space, we apply the operator $\mathbf{n}_S \cdot \nabla(\cdot)$ to Eq. (25). After some convenient arrangements, this yields

$$\frac{\partial g_S}{\partial t} = -\mathbf{u}\cdot\nabla g_S + g_S a_S + \frac{\partial \Gamma_S}{\partial n_S}, \tag{26}$$

where $a_S = -\mathbf{n}_S \cdot \partial\mathbf{u}/\partial n_S\cdot$, with $\mathbf{n}_S = \nabla S/|\nabla S|$ denoting an unit vector normal to the isosurface of S. A more detailed derivation of the g_S-equation is given in Appendix A. Now, making use of the Lagrangian interpretation of the temporal derivative in composition space, Eq. (9), we have

$$\frac{\partial g_S}{\partial \tau} = \frac{\partial g_S}{\partial t} + \mathbf{u}_p \cdot \nabla g_S. \tag{27}$$

Inserting Eq. (26) into Eq. (27), and making use of both the expression for the particle velocity, Eq. (7), and the transformation rule, Eq. (11), we obtain

$$\frac{\partial g_S}{\partial \tau} = -\Gamma_Z \frac{\partial g_S}{\partial Z} - \Gamma_\varphi \frac{\partial g_S}{\partial \varphi} + g_S a_S + \frac{\partial \Gamma_S}{\partial n_S}. \tag{28}$$

Additionally, using the following mathematical identity

$$\frac{\partial \Gamma_S}{\partial n_S} = g_S \frac{\partial}{\partial n_S}\left(\frac{\Gamma_S}{g_S}\right) + \frac{\Gamma_S}{g_S}\frac{\partial g_S}{\partial n_S}, \tag{29}$$

we can rewrite Eq. (28) as

$$\frac{\partial g_S}{\partial \tau} = -\Gamma_Z \frac{\partial g_S}{\partial Z} - \Gamma_\varphi \frac{\partial g_S}{\partial \varphi} + g_S a_S + g_S^2 \frac{\partial}{\partial S}\left(\frac{\Gamma_S}{g_S}\right) + \Gamma_S \frac{\partial g_S}{\partial S}. \tag{30}$$

It is interesting to note at this point, that once Eq. (30) is specialized either for Z or φ, a tangential derivative will remain, which differs from previous formulations for g_Z and g_c derived for the classical non-premixed and premixed asymptotic limits [24, 4, 14, 22, 29]. Also, this result is not compatible with the use of simple analytical expressions for the closure of the conditioning scalar gradients typically having a one-dimensional dependency in composition space. With Eq. (30), the component C_3 of the aimed composition space theory has been specified.

3. Solvable system of equations for unity Lewis number

In the previous section, the components C_1, C_2 and C_3 explained in the introduction have been specified. The resulting set of equations, however, is not written in a solvable form. In order to illustrate how a closed and solvable formulation can be obtained, we proceed now to specialize the equations derived in Section 2. For simplicity, unity Lewis number will be assumed here, but we remark that the formulation presented so far is general and that it can be directly used in non-unity Lewis number situations, too. The equations obtained in this section correspond to the component C_4 specified in the introduction.

3.1. Composition space equations for chemical species and temperature

We proceed now to specialize Eq. (13) for chemical species, Y_k, and temperature, T. These quantities are assumed to be governed by

$$\frac{\partial Y_k}{\partial t} + \mathbf{u}\cdot\nabla Y_k = \frac{1}{\rho}\nabla\cdot(\rho D \nabla Y_k) + \frac{\dot{\omega}_k}{\rho} \tag{31}$$

and

$$\frac{\partial T}{\partial t} + \mathbf{u}\cdot\nabla T = \frac{1}{\rho}\nabla\cdot(\rho D \nabla T) + \frac{D}{c_p}\nabla T\cdot\nabla c_p + \frac{\dot{\omega}_T}{\rho} + \sum_{k=1}^{N}\frac{c_{p,k}}{c_p} D \nabla Y_k\cdot\nabla T, \tag{32}$$

respectively. In Eqs. (31) and (32), ρ is the density, D is a diffusion coefficient, $\dot{\omega}_k$ is a mass source term of species k due to chemical reaction and $\dot{\omega}_T$ is a corresponding energy source term. Additionally, $c_{p,k}$ and c_p are the specific heat capacity at constant pressure of species k and of the mixture, respectively. While Eqs. (31) and (32) formally specify Γ_{Y_k} and Γ_T, we still need explicit forms for Γ_Z and Γ_φ. The former is specified by means of the transport equation of the mixture fraction, which is assumed here to have the following form

$$\frac{\partial Z}{\partial t} + \mathbf{u}\cdot\nabla Z = \frac{1}{\rho}\nabla\cdot(\rho D\nabla Z)\,. \tag{33}$$

For Γ_φ, on the other hand, an expression can be directly obtained by means of Eq. (23), provided that Γ_c is first specified. Assuming that Y_c is governed by

$$\frac{\partial Y_c}{\partial t} + \mathbf{u} \cdot \nabla Y_c = \frac{1}{\rho} \nabla \cdot (\rho D \nabla Y_c) + \frac{\dot{\omega}_c}{\rho}, \tag{34}$$

and making use of the transformation rule, Eq. (11), and Eq. (15) to rewrite the RHS as

$$\begin{aligned} \Gamma_c &= \frac{1}{\rho} \left[\nabla \cdot (\rho D \nabla Y_c) + \dot{\omega}_c \right] \\ &= \frac{1}{\rho} \left[\nabla \cdot (\rho D \nabla \varphi) + \rho D |\nabla Z|^2 \frac{\partial^2 Y_c}{\partial Z^2} + \nabla \cdot (\rho D \nabla Z) \frac{\partial Y_c}{\partial Z} + \dot{\omega}_c \right], \end{aligned} \tag{35}$$

we can obtain the following transport equation for φ from Eq. (24)

$$\frac{\partial \varphi}{\partial t} + \mathbf{u} \cdot \nabla \varphi = \frac{1}{\rho} \nabla \cdot (\rho D \nabla \varphi) + \frac{\dot{\omega}_\varphi}{\rho}, \tag{36}$$

where

$$\dot{\omega}_\varphi = \rho D |\nabla Z|^2 \frac{\partial^2 Y_c}{\partial Z^2} + \dot{\omega}_c. \tag{37}$$

With Γ_{Y_k}, Γ_T, Γ_Z and Γ_φ already specified, and after application of the above-defined transformation rules, Eq. (11), we can obtain now specific composition space equations for chemical species and temperature. These yield

$$\rho \frac{\partial Y_k}{\partial \tau} + \frac{\partial Y_k}{\partial \varphi} \dot{\omega}_\varphi = \rho D g_Z^2 \frac{\partial^2 Y_k}{\partial Z^2} + \rho D g_\varphi^2 \frac{\partial^2 Y_k}{\partial \varphi^2} + \dot{\omega}_k \tag{38}$$

and

$$\begin{aligned} \rho \frac{\partial T}{\partial \tau} + \frac{\partial T}{\partial \varphi} \dot{\omega}_\varphi = {} & \rho D g_Z^2 \frac{\partial^2 T}{\partial Z^2} + \rho D g_\varphi^2 \frac{\partial^2 T}{\partial \varphi^2} + \frac{\rho D}{c_p} \left[g_Z^2 \frac{\partial T}{\partial Z} \frac{\partial c_p}{\partial Z} + g_\varphi^2 \frac{\partial T}{\partial \varphi} \frac{\partial c_p}{\partial \varphi} \right] \\ & + \sum_{k=1}^{N} \frac{c_{p,k}}{c_p} \left[\rho D g_Z^2 \frac{\partial Y_k}{\partial Z} \frac{\partial T}{\partial Z} + \rho D g_\varphi^2 \frac{\partial Y_k}{\partial \varphi} \frac{\partial T}{\partial \varphi} \right] + \dot{\omega}_T, \end{aligned} \tag{39}$$

respectively. A detailed explanation of the transformation of Γ_{Y_k} and Γ_T is given in Appendix C. In the next section, the g_S-equation will be specialized for g_Z and g_φ.

3.2. The scalar gradient equations

Considering Eqs. (33) and (36), Γ_Z and Γ_φ can be generalized as

$$\begin{aligned} \Gamma_S &= \frac{1}{\rho} \nabla \cdot (\rho D \nabla S) + \frac{\delta_{\varphi S} \dot{\omega}_S}{\rho} \\ &= \frac{1}{\rho} \frac{\partial}{\partial n_S} (\rho D g_S) - D g_S \kappa_S + \frac{\delta_{\varphi S} \dot{\omega}_S}{\rho}, \end{aligned} \tag{40}$$

where $\kappa_S = -\nabla \cdot \mathbf{n}_S$ is the curvature associated with the S-isosurface and $\delta_{\varphi S}$ is the Kronecker delta function, which adopts a value of 1 for $S = \varphi$ and 0 for $S = Z$. With this, we can rewrite part of the fourth term in the right hand side of Eq. (30) as

$$\frac{\partial}{\partial S}\left(\Gamma_S/g_S\right) = \frac{1}{\rho}\frac{\partial^2}{\partial S^2}\left(\rho D g_S\right) - \frac{1}{\rho^2}\frac{\partial \rho}{\partial S}\frac{\partial}{\partial S}\left(\rho D g_S\right) - \frac{\partial}{\partial S}\left(D\kappa_S\right) + \frac{\partial}{\partial S}\left(\frac{\delta_{\varphi,S}\dot{\omega}_S}{\rho g_S}\right). \tag{41}$$

Inserting Eq. (41) into Eq. (30), and specializing for $S = Z$ and $S = \varphi$, we obtain

$$\begin{aligned}\frac{\partial g_Z}{\partial \tau} = &-\left[\frac{g_\varphi}{\rho}\frac{\partial}{\partial \varphi}\left(\rho D g_\varphi\right) - D g_\varphi \kappa_\varphi + \frac{\dot{\omega}_\varphi}{\rho}\right]\frac{\partial g_Z}{\partial \varphi} \\ &+ \frac{g_Z^2}{\rho}\frac{\partial^2}{\partial Z^2}\left(\rho D g_Z\right) - \frac{g_Z^2}{\rho^2}\frac{\partial \rho}{\partial Z}\frac{\partial}{\partial Z}\left(\rho D g_Z\right) \\ &- g_Z^2\frac{\partial}{\partial Z}\left(D\kappa_Z\right) + g_Z a_Z\end{aligned} \tag{42}$$

and

$$\begin{aligned}\frac{\partial g_\varphi}{\partial \tau} = &-\left[\frac{g_Z}{\rho}\frac{\partial}{\partial Z}\left(\rho D g_Z\right) - D g_Z \kappa_Z\right]\frac{\partial g_\varphi}{\partial Z} \\ &+ \frac{g_\varphi^2}{\rho}\frac{\partial^2}{\partial \varphi^2}\left(\rho D g_\varphi\right) - \frac{g_\varphi^2}{\rho^2}\frac{\partial \rho}{\partial \varphi}\frac{\partial}{\partial \varphi}\left(\rho D g_\varphi\right) \\ &- g_\varphi^2\frac{\partial\left(D\kappa_\varphi\right)}{\partial \varphi} + g_\varphi^2\frac{\partial}{\partial \varphi}\left(\frac{\dot{\omega}_\varphi}{\rho g_\varphi}\right) + g_\varphi a_\varphi,\end{aligned} \tag{43}$$

respectively, where use of Eq. (40) has been made. With Eqs. (42) and (43), the composition space equations for chemical species and temperature, Eqs. (38) and (39), are closed provided the strain rates, a_Z and a_φ, and the curvatures, κ_Z and κ_φ, can be properly modelled. This set of equations represents the component C_4 of the aimed composition space theory.

4. Assessment framework

In this section, an appropriate framework for the study of partially premixed combustion effects is provided together with a numerical approach for the solution of the equations obtained in the previous section. These elements represent the basis for the component C_5 of the aimed composition space theory.

4.1. Demonstration case

As a demonstration case, we choose the flame-tangential interaction between premixed flamelets with different equivalence ratios (ϕ =0.5-1.7, CH_4-air, p = 1 atm, T_0 = 300 K). This scenario mimics a flame-front propagating into a stratified mixture of fresh reactants. Both curvature effects

and the influence of strain on the g_φ-equation are neglected for simplicity and only steady state solutions are analyzed. The interaction between the premixed flamelets is controlled by the strain rate imposed for the g_Z-equation which is discussed further below.

Figure 1 shows a schematic of the computational domain together with the initialization and the boundary conditions. The Z and φ dimensions are normalized according to

$$Z^*(Z) = \frac{Z - Z_{\min}}{Z_{\max} - Z_{\min}} \tag{44}$$

and

$$\varphi^*(Z, \varphi) = \frac{\varphi - \varphi_{\min}}{\varphi_{\max}(Z) - \varphi_{\min}}, \tag{45}$$

respectively. Utilizing the (Z^*, φ^*)-space allows an advantageous implementation of the numerical solution algorithm solving the equations on a unit square grid (further details are provided in Sec. 4.2). Note that the mixture fraction is normalized due to the fact that the left and right boundary conditions correspond to lean ($\phi = 0.5$, $Z_{\min} = 0.0284$) and rich mixtures ($\phi = 1.7$, $Z_{\max} = 0.0903$), respectively, and not to pure oxidizer and fuel. Even though we present this normalization for a specific case here, we emphasize that it could analogously be applied for other, more general cases.

For temperature and species, cold mixing between the lean and the rich mixture is prescribed as boundary condition at $\varphi* = 0$. For the left ($Z^* = 0$), lean and rich premixed flamelet solutions are chosen, respectively. At the top boundary ($\varphi^* = 1$) a non-premixed flame with an imposed strain rate is prescribed.

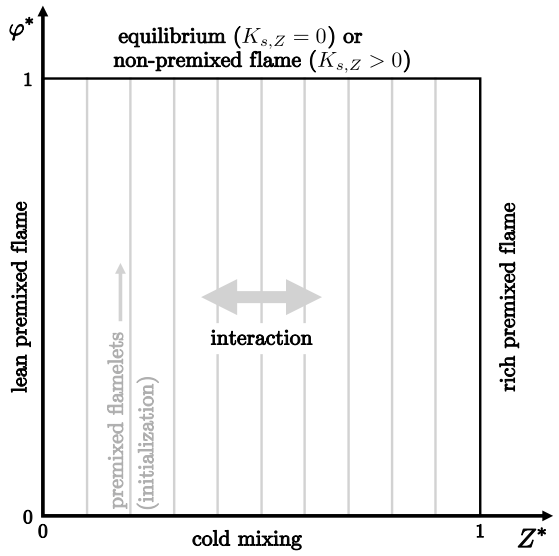

Figure 1: Schematic of the (Z^*, φ^*) computational domain.

In order to introduce the assumptions adopted above, it is convenient to replace the strain rates a_Z and a_φ by $K_{s,Z}$ and $K_{s,\varphi}$, respectively, where

$$K_{s,S} = -\frac{1}{\rho}\frac{\partial}{\partial n_S}\left(\frac{\rho\,\Gamma_S}{g_S}\right), \tag{46}$$

with S denoting either Z or φ. This expression stems from the definition of strain usually employed in strong stretch theory [30, 31]. According to the recent work by Olguin et al. [29], but using the notation adopted in the present work, the relation between the both possible definitions of strain is

$$g_S a_S = g_S K_{s,S} + \frac{\partial g_S}{\partial \tau} + \frac{\Gamma_S}{\rho}\frac{\partial \rho}{\partial n_S}. \tag{47}$$

For the cases under consideration, Eq. (47) leads to

$$a_Z = K_{s,Z} + \left[g_Z \frac{\partial}{\partial Z}\left(\rho D g_Z\right)\right]\frac{1}{\rho^2}\frac{\partial \rho}{\partial Z}, \tag{48}$$

$$a_\varphi = \left[g_\varphi \frac{\partial}{\partial \varphi}\left(\rho D g_\varphi\right) + \dot{\omega}_\varphi\right]\frac{1}{\rho^2}\frac{\partial \rho}{\partial \varphi}, \tag{49}$$

which formalizes $K_{s,Z}$ as the only free parameter controlling the interaction between the unstretched premixed flamelets.

The analysis starts considering (one-dimensional, non-interacting) premixed flamelet solutions corresponding to the local mixture fraction. For this situation, $K_{s,Z} = 0$, which implies that the mixture stratification vanishes in the entire domain ($g_Z = 0$). Accordingly, in this case the solver reduces to a solution algorithm for non-interacting unstretched premixed flamelets [8] and the top boundary condition simplifies to the chemical equilibrium corresponding to the local mixture fraction. Other cases are then generated by keeping all boundary conditions considered in the first case, but increasing the strain rate, $K_{s,Z}$. In particular, a constant $K_{s,Z}$ is imposed in the entire domain (including the bottom and top boundary conditions), which introduces important tangential interactions between the different originally non-interacting premixed flamelets.

It should be noted that the concept of interacting premixed flamelets is just one interpretation of the flame which is employed here for illustrative purposes. In general, the two-dimensional composition space formulation does not rely on a (one-dimensional) flamelet representation for the flame, even though one-dimensional premixed and non-premixed flamelet equations can be recovered as limiting cases. We emphasize that multi-regime combustion characteristics arise in many different flame configurations, as discussed in detail in the literature, see for instance [32, 19, 16, 22]. The representation of other flame configurations in two-dimensional composition space depends on the choice of the boundary conditions and the flame parameters, which will be explored in future work.

4.2. Transformation rules

Solving the composition space equations on the (Z^*, φ^*)-grid requires a change in variables and the reformulation of all terms according to the respective transformation rules, Eqs. (44) and (45). The partial derivatives with respect to Z and φ are readily rewritten as

$$\frac{\partial(\cdot)}{\partial Z} = \frac{1}{\Delta Z}\frac{\partial(\cdot)}{\partial Z^*} - \frac{\varphi^*}{\Delta\varphi}\frac{\partial\varphi_{\max}}{\partial Z}\frac{\partial(\cdot)}{\partial\varphi^*} \tag{50}$$

and

$$\frac{\partial(\cdot)}{\partial\varphi} = \frac{1}{\Delta\varphi}\frac{\partial(\cdot)}{\partial\varphi^*}, \tag{51}$$

respectively, where $\Delta Z = Z_{\max} - Z_{\min}$ and $\Delta\varphi = \varphi_{\max}(Z) - \varphi_{\min}$. Further details about this transformation are provided in Appendix D. Considering the simplistic transformation rule for Z, some readers might find it surprising that its partial derivatives are replaced by a combination of both partial derivatives with respect to Z^* and φ^*. This aspect can be understood from the stretching of the space in the vertical direction, which is shown in Fig. 2. Keeping in mind that a partial differentiation with respect to Z^* implies φ^* is held constant, which corresponds to a horizontal direction in Fig. 2 (left), the bending of the iso-φ^* gridlines in Fig. 2 (right) clearly shows that the differentiation with respect to Z (i. e. with φ held constant) demands an additional term describing the grid deformation. The latter depends on the upper bound $\varphi = \varphi_{\max}(Z)$, which appears in the second term in Eq. (50). On the other hand, differentiating with respect to φ (i. e. along the vertical direction in Fig. 2) leads to a simple re-scaling of the partial derivative with respect to φ^*.

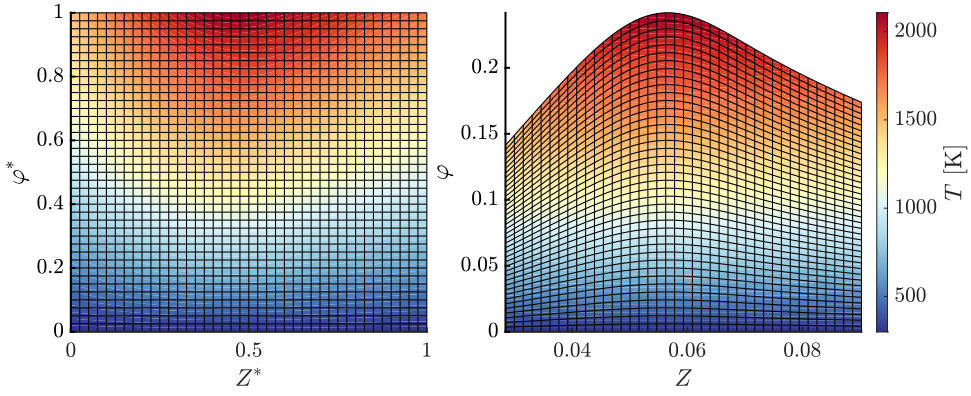

Figure 2: Mapping of the scalar temperature field, computed on an orthogonal grid in (Z^*, φ^*)-space, to (Z,φ)-space. The formulation of the 2D composition space equations with respect to the computational (Z^*, φ^*)-domain requires a change of variables as described in Sec. 4.2 and Appendix D.

Transforming the second partial derivatives with respect to Z and φ, one obtains

$$\frac{\partial^2(\cdot)}{\partial Z^2} = \frac{1}{(\Delta Z)^2}\frac{\partial^2(\cdot)}{\partial Z^{*2}} + m_1\frac{\partial^2(\cdot)}{\partial\varphi^*\partial Z^*} + m_2\frac{\partial^2(\cdot)}{\partial\varphi^{*2}} + m_3\frac{\partial(\cdot)}{\partial\varphi^*} \tag{52}$$

and

$$\frac{\partial^2(\cdot)}{\partial\varphi^2} = \frac{1}{(\Delta\varphi)^2}\frac{\partial^2(\cdot)}{\partial\varphi^{*2}}, \tag{53}$$

with

$$m_1 = -2\frac{\varphi^*}{\Delta\varphi\Delta Z}\frac{\partial\varphi_{\max}}{\partial Z},$$

$$m_2 = \frac{\varphi^{*2}}{(\Delta\varphi)^2}\left(\frac{\partial\varphi_{\max}}{\partial Z}\right)^2,$$

and

$$m_3 = \frac{2\varphi^*}{(\Delta\varphi)^2}\left(\frac{\partial\varphi_{\max}}{\partial Z}\right)^2 - \frac{\varphi^*}{\Delta\varphi}\frac{\partial^2\varphi_{\max}}{\partial Z^2}.$$

The above transformation rules need to be carefully introduced for all partial derivatives of thermochemical scalars appearing in derived the composition space equations. It is noted that the transformation introduces cross derivatives according to Eq. (52), which can be computed on the numerical grid, but no cross scalar dissipation rates, such that no further modeling efforts are required. The formulation of the fully transformed equations in terms of Z^* and φ^* is provided in Appendix E.

4.3. Solution algorithm

The equations for temperature, species and the gradients g_Z and g_φ are solved with an alternating direction implicit (ADI) scheme according to Douglas and Gunn [33]. With this method, two tridiagonal matrixes are solved in every time step and the overall numerical solution is advanced until convergence to a steady state. The steady state is verified by two measures: (i) temporal derivatives of solution quantities are smaller than a prescribed threshold value and (ii) probes throughout the two-dimensional domain confirm that the overall solution remains invariant with further integration in τ. The grid resolution is set to 100 grid points in both dimensions. All species' thermodynamic properties, transport coefficients, and chemical source terms are evaluated with cantera [34] and a reduced GRI 3.0 mechanism (28 species, 112 reactions) is adopted for the description of chemical reactions [35].

5. Results and discussion

In this section, we analyze numerical solutions of the 2D composition space equations. For the demonstration case, a parameter variation of the strain rate $K_{s,Z}$ between 0/s and 200/s is performed, which can be understood as increasing interactions between initially separated premixed flamelets, as previously stated. First, the response of the flame structure to this strain variation is examined. Thereafter, a budget analysis of the novel gradient equations is performed. The section concludes with a discussion of how the numerical approach could be integrated into existing state-of-the-art simulation frameworks. With this analysis, the component C_5 of the aimed theory is completed.

5.1. Flame structure and the effect of strain

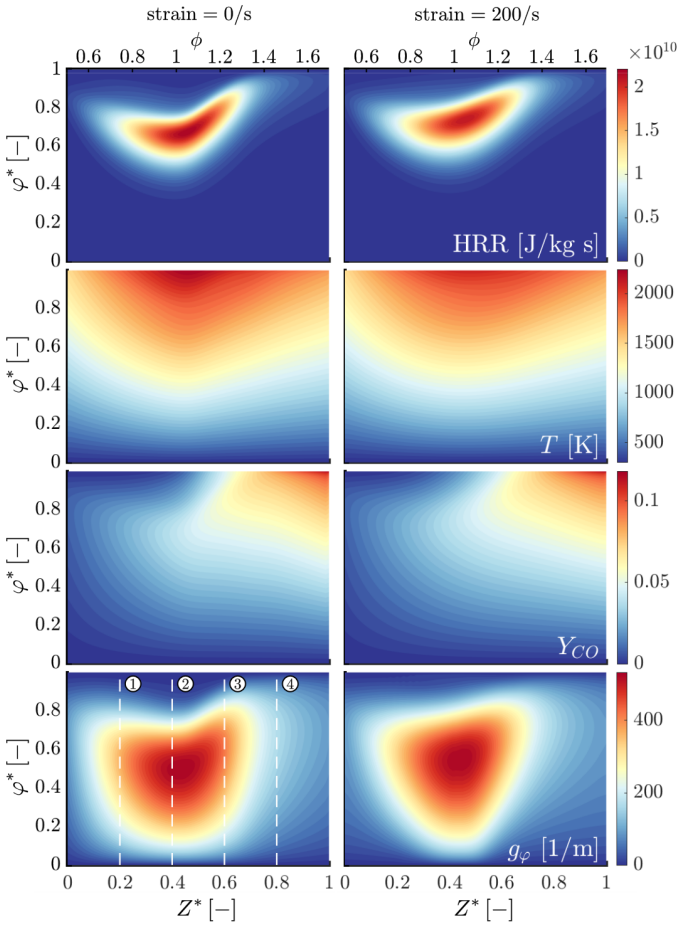

Figure 3: Contours for the solution quantities heat release rate (HRR), temperature T, mass fraction Y_{CO}, and the gradient g_φ in (Z^*, φ^*)-space. For orientation, the local equivalence ratio, ϕ, is plotted as a second axis on top.

The solution for selected thermochemical scalars is analyzed first by means of contours (Fig. 3) and then for individual profiles along vertical slices in the (Z^*, φ^*)-space (Fig. 4). From top to

bottom, Fig. 3 shows the heat release rate (HRR), the temperature, the mass fraction of CO and the gradient g_φ. Note that the local equivalence ratio is plotted as a second axis on top of Fig. 3 to aid the interpretation of the results. Inspecting the contour plot of the HRR (Fig. 3, top row), the region with relevant heat release first exhibits a v-shape which becomes a disk shape towards higher strain rates. Furthermore, the lower edge of this region moves slightly towards higher φ^*. For the temperature (Fig. 3, second row), small changes are observed around stoichiometry ($\phi = 1$, as indicated on the top axis), where the temperature slightly decreases with increasing strain. Other than that, visual differences in the contour plot remain small, which also applies for the species CO (Fig. 3, third row). In contrast, the gradient g_φ (Fig. 3, bottom row) shows a notable response to the strain variation. The high-gradient region initially exhibits a u-shape, which becomes a v-shape towards higher strain rates.

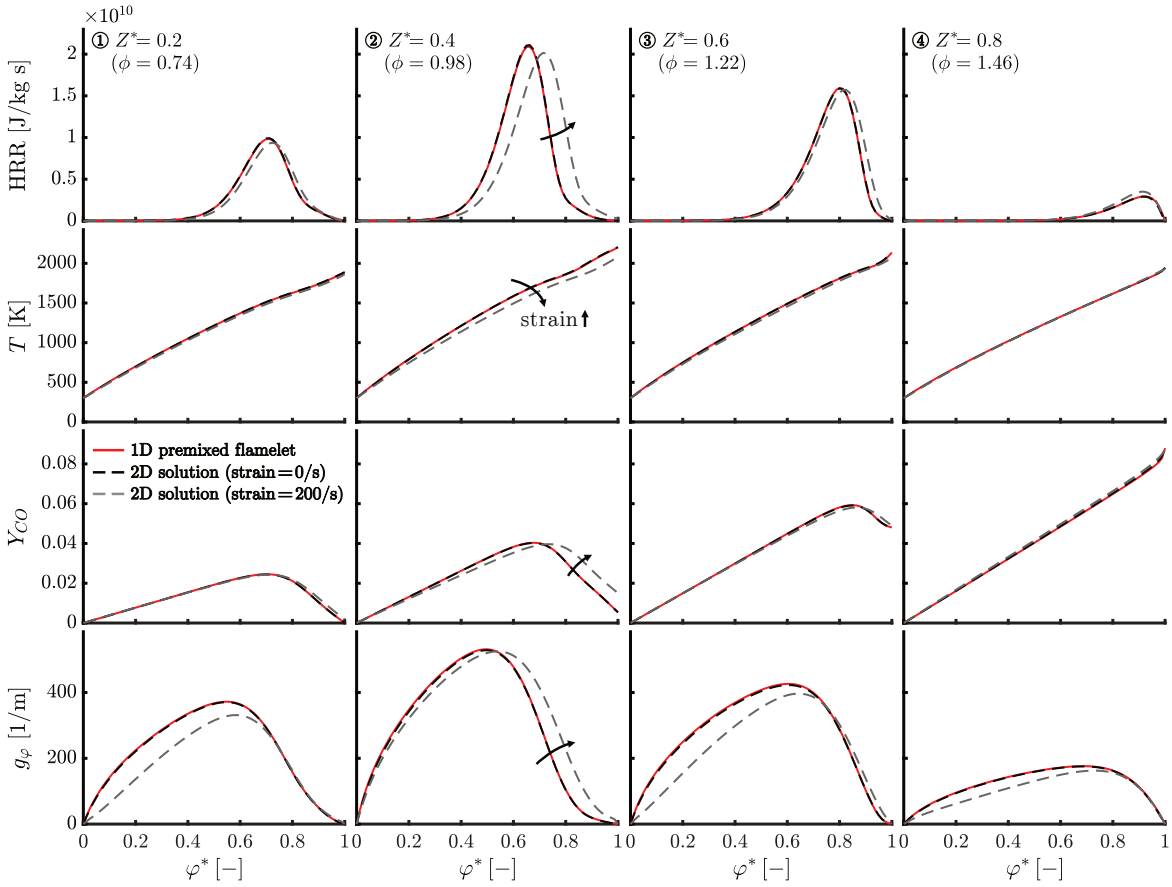

Figure 4: Profiles of the solution quantities heat release rate (HRR), temperature T, mass fraction Y_{CO}, and the gradient g_φ along four vertical slices in (Z, φ^*)-space (dashed lines). The vertical slices are also marked in Fig. 3. All profiles are colored according to the strain value prescribed for the 2D solution and brighter grey colors correspond to a higher strain value. For reference, corresponding profiles of a 1D unstretched premixed flamelet are shown (red solid line).

For a more detailed inspection of the solution quantities, their profiles are extracted and compared along four vertical slices ($Z^* = 0.2/.4/.6/.8$) which are indicated in the lower left contour plot in Fig. 3. The solution profiles along these four vertical slices are plotted in Fig. 4 (left to right). The black dashed line corresponds to zero strain, while grey corresponds to an elevated strain rate of 200/s. Furthermore, the solution for a 1D unstretched premixed flame, which corresponds to the local mixture fraction Z^* in each column, is plotted for reference. Notably, the zero strain solutions are in perfect agreement with the 1D flamelet solution which confirms the recovery of the premixed limit. It is further found that all solution quantities are affected by the flamelet-to-flamelet interaction close to stoichiometry (Fig. 4, second column). On the lean side ($Z^* = 0.2$, first column) the gradient g_φ shows a clear response to the strain variation, while the HRR shows a small but notable shift to higher φ^*, and the other solution quantities remain mostly unaffected. On the rich side ($Z^* = 0.6/0.8$), the gradient g_φ changes significantly and the HRR again shows a minor response to strain while T and Y_{CO} show almost no changes. In summary, the interaction between neighbouring premixed flamelets starts to affect the stoichiometric region first, similar to the response of non-premixed flames to strain. Increasing the strain rate, also lean and rich regions become more and more affected. Since the largest variation of the thermochemical scalars, and the flames' reactivity in general, are found in the vicinity of stoichiometry, this behaviour appears conceivable. The observations further illustrate how the 2D model combines properties of both, premixed and non-premixed flames, which is characteristic for partially premixed/multi-regime combustion.

5.2. Budget analysis for the gradient equations

Figure 5 shows the budgets of the gradient equations, Eqs. (42) and (43), for a 2D solution with an intermediate strain rate of 100/s. All terms of the equations are evaluated along a vertical slice ($Z^* = 0.3$) and a horizontal slice ($\varphi^* = 0.8$) of the (Z^*, φ^*)-domain, and they are shown in the middle and on the ride side of Fig. 5, respectively. The slices are marked in the contour plots of the gradients g_Z (top) and g_φ (bottom) on the left of the figure. For reference, the gradient equations are shown with all relevant terms above the plots for the readers convenience. Inspecting the g_Z equation budgets, it is found that the diffusion terms mainly balance the φ-convection term[1], with a smaller but non-negligible contribution to the overall budget from the strain term. This marks a significant difference to purely non-premixed flames, for which the φ-convection term does not exist and where the diffusive terms consequently only compensate the strain term. As can be observed

[1]Terms which contain a first derivative of the corresponding solution quantity are formally interpreted as convective terms in composition space.

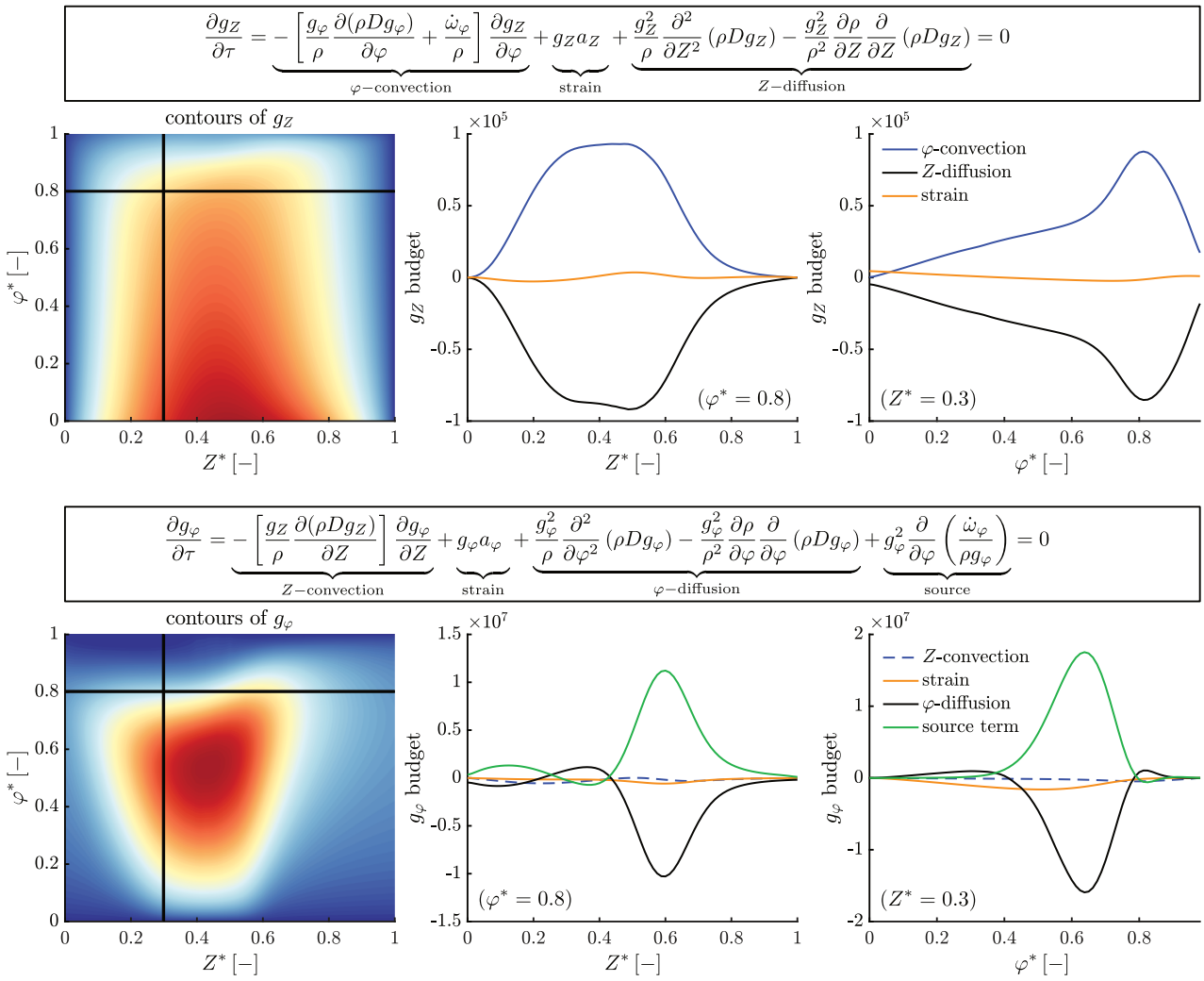

Figure 5: Left: contour plots of the gradients $g_Z = |\nabla Z|$ and $g_\varphi = |\nabla \varphi|$ corresponding to a 2D composition space solution with strain=100/s. Budgets of the gradient equations are shown along horizontal slices ($\varphi^* = 0.8$, middle) and vertical slices ($Z^* = 0.3$, right). For the readers convenience, the simplified Eqs. (42) and (43) are shown above each plot indicating the individual terms.

from its contour plot, g_Z is large at the lower boundary and smaller at the top boundary, which shows that the g_Z information prescribed at the lower boundary is propagated into the domain by means of this φ-convection term (the term is positive everywhere). Hence, the interaction term represents an important mechanism, distributing gradient information in the 2D composition space.

Considering the g_φ equation budgets, primarily the φ-diffusion term and the source term, which originates from chemical reactions, balance each other. These terms are also present in the gradient equations for purely premixed flames [9]. Notably, the Z-convection term, which is a novel characteristic for the 2D formulation, shows an almost negligible influence for the slice $\varphi^* = 0.8$. This is consistent with Fig. 4, which confirms that the g_φ-profiles are almost unaffected by the imposed

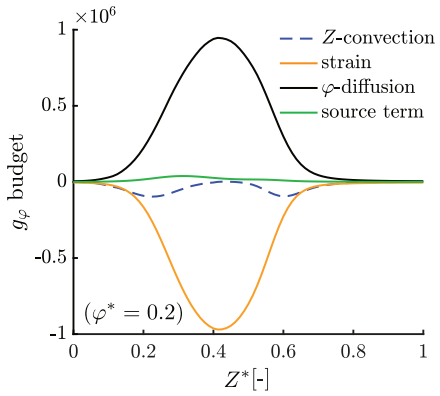

Figure 6: Budget of the g_φ-equation along a horizontal slice ($\varphi^* = 0.2$) corresponding to a 2D composition space solution with strain=100/s. The terms are denoted analogously to Fig. 5.

strain (i. e. flamelet-flamelet interactions) for $\varphi^* > 0.5$. Extracting an additional horizontal slice at $\varphi^* = 0.2$, the budgets appear different, cf. Fig. 6. Consistently with findings of the previous section, which showed notable influence of the flamelet-flamelet interactions on g_φ in the region $\varphi^* < 0.5$, now the strain term balances the φ-diffusion term with small, but non-negligible contributions from the source and the Z-convection term. Furthermore, the budget terms are an order of magnitude smaller. This is due to the fact that the progress variable source term, which appears similar to the HRR shown in Fig. 3, dominates the equation budgets where it is large (around stoichiometry and for $\varphi^* > 0.5$). It should further be noted that the gradients g_Z and g_φ are large in this area, which therefore corresponds to a confined region of high chemical activity in the physical space. Away from this region of high chemical reactivity, flamelet-flamelet interactions show a pronounced effect on the 2D composition space solution and it can be expected that this effect becomes stronger for higher imposed strain rates.

6. Conceivable coupling strategy to CFD-codes

To this point, we presented a closed system of composition space equations and demonstrated their numerical solution by a suitable algorithm. With only few parameters and an adequate definition of boundary conditions, the overall approach can serve as a basis for modeling multi-regime combustion when coupled to a flow solver. In this section, we outline such a coupling strategy and discuss its strength and open issues left to implement it, all from a conceptual perspective.

Considering large eddy simulation (LES) approaches operating with tabulated manifolds, it appears attractive to project the composition space solution into the conventional (Z,Y_c)-space. This allows utilizing exisiting subgrid scale closures based on progress variable and mixture fraction, such as presumed PDF [17, 36] or artificial thickened flame (ATF) approaches [37]. To date, tabulated

manifolds are often generated either from premixed or non-premixed flamelets (i. e., the limiting cases) and have already been used for partially premixed / multi-regime combustion simulations with reasonable results [32, 38, 39]. Hence, it is conceivable that the aforementioned coupling strategies can also be applied with minor modifications to the current modeling approach. In this context, it is important to differentiate between Z^* and φ^* (Eq. (44)), which are useful normalized coordinates to solve the 2D composition space equations, and the conventional Z and Y_c, which appear more beneficial to parameterize a manifold and couple it to a CFD code. Besides Z and Y_c, at least a third quantity is required for the parameterization of the manifold to reflect the imposed strain rate, which itself controls the extent of mixture stratification and flamelet-flamelet interactions. However, in opposition to previous coupling approaches, it would not be necessary to provide an ad-hoc model to bridge between the strain rate imposed to the scalar field by turbulence and the scalar gradients (or the scalar dissipation rates). Instead with the present formulation, the scalar gradients are explicitly computed in composition space, with the strain rate being a direct input flow parameter of the modeling. The SGS modeling would then need to focus on the fluctuating part of the strain rate, a quantity which has deserved attention in the context of flame surface density modeling [40].

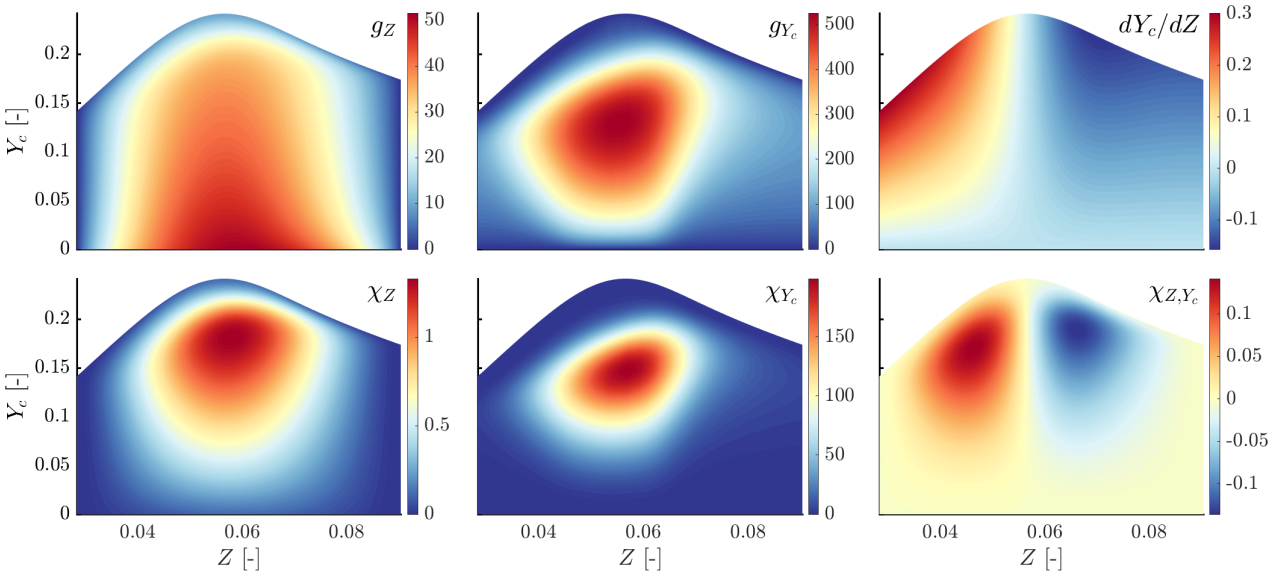

Figure 7: 2D composition space solution (strain=100/s) projected into (Z, Y_c)-space. The figure shows the gradients and scalar dissipation rates for the mixture fraction and the reaction progress variable together with the reconstructed cross-terms $\partial Y_c/\partial Z$ and χ_{Z,Y_c}. The latter terms can be directly computed from the numerical solution of the 2D composition space solution.

To illustrate the potential of the proposed strategy, Figure 7 shows the projection of a 2D

composition space solution into (Z,Y_c)-space. The projection is readily obtained calculating Y_c as a weighted sum of species and utilizing the backward transformation $Z^* \rightarrow Z$, cf. Eq. (44). From the numerical solution of the mixture fraction gradient, g_Z, the composition-space distribution of the scalar dissipation rate, $\chi_Z = 2Dg_Z^2$, can be determined. The progress variable gradient, $g_c = |\nabla Y_c|$, is not a solution quantity, but it can be computed as [22]

$$g_c^2 = g_\varphi^2 + g_Z^2 \left(\frac{\partial Y_c}{\partial Z} \right)^2 . \tag{54}$$

Analogously, the scalar dissipation rate of the progress variable is obtained from $\chi_{Y_c} = 2Dg_c^2$. These scalar dissipation rates provide estimations of SGS scalar mixing frequencies useful in scalar SGS mixing modeling [41].

Employing orthogonal coordinates, χ_{Z,Y_c} does not appear in the equations and can be retrieved by post processing the numerical solution [22]

$$\chi_{Z,Y_c} = 2Dg_Z^2 \frac{\partial Y_c}{\partial Z} . \tag{55}$$

While this quantity explicitly requires a closure in other 2D composition space approaches [24, 19, 21], this is not the case for the present model. Interestingly, due to the fact that χ_{Z,Y_c} contains information on both orientation and magnitude of ∇Z and ∇Y_c, it will qualify to help improving the modeling. This will be particularly the case using probability density functions to calibrate the SGS correlations between mixture fraction and progress of reaction. These unresolved correlations are linked to fluctuations whose amplitude can be expected to depend on the topology of the multi-regime reaction zones, topology which, on the other hand, directly relates to the cross-scalar dissipation rate $\chi_{Z,Y_c} = 2D\nabla Z \cdot \nabla Y_c$.

7. Conclusions

In this work, it has been shown how adopting a Lagrangian interpretation of the flamelet transformation allows deriving a self-consistent set of two-dimensional composition space equations for partially premixed combustion. The formulation makes use of the mixture fraction, Z, and a modified reaction progress variable, φ, where the latter is defined in such a way that the condition $\nabla Z \cdot \nabla \varphi = 0$ is satisfied in the entire flame domain. Additionally to the typical composition space equations for chemical species and temperature, equations for $g_Z = |\nabla Z|$ and $g_\varphi = |\nabla \varphi|$ were derived, which allowed to achieve a solvable formulation in terms of four parameters: two strain rates (a_Z, a_φ) and two curvatures (κ_Z, κ_φ). After an appropriate numerical approach was introduced, the derived set of 2D equations was employed to study the interaction between premixed flamelet

structures subject to different levels of imposed strain in the Z-direction. A budget analysis of the different contributions to the scalar gradient equations showed that for g_Z, diffusion is mainly balanced by convection in the φ-direction. The latter effect is not included in previous g-equations obtained in the context of single-regime combustion, which highlights the relevance of the current extended formulation. For g_φ, on the other hand, it was found that diffusion is mainly balanced by terms associated with chemical reactions. This roughly coincides with results obtained for the gradient of the conventional reaction progress variable in the context of premixed flames, even when some influence of the interaction between flamelets could be observed. These results provide new and important insights into the physics of scalar gradients in two-dimensional composition space equations. Finally, conceivable coupling strategies of the present formulation with CFD codes were discussed in the context of the numerical simulation of turbulent flames.

Acknowledgments

Part of the work was funded by the Deutsche Forschungsgemeinschaft (DFG, German Research Foundation) – Projektnummer 325144795.

Appendix A. Derivation of the g_S-equation

For the derivation of a general equation for g_S, we apply the operator $\mathbf{n}_S \cdot \nabla(\cdot)$ to Eq. (13), which yields

$$\mathbf{n}_S \cdot \nabla \left(\frac{\partial S}{\partial t} + \mathbf{u} \cdot \nabla S = \Gamma_S \right). \tag{A.1}$$

The transient term can be then rewritten as

$$\begin{aligned} \mathbf{n}_S \cdot \nabla \left(\frac{\partial S}{\partial t} \right) &= n_i \frac{\partial}{\partial x_i} \left(\frac{\partial S}{\partial t} \right) \\ &= n_i \frac{\partial}{\partial t} \left(|\nabla S| n_i \right) \\ &= \underbrace{n_i n_i}_{=1} \frac{\partial g_S}{\partial t} + g_S \underbrace{n_i \frac{\partial n_i}{\partial t}}_{=0} \\ &= \frac{\partial g_S}{\partial t}, \end{aligned} \tag{A.2}$$

while the convective term yields

$$\begin{aligned}\mathbf{n}_S \cdot \nabla \left(\mathbf{u} \cdot \nabla S\right) &= n_i \frac{\partial}{\partial x_i}\left(u_j \frac{\partial S}{\partial x_j}\right) \\ &= n_i u_j \frac{\partial}{\partial x_j}\left(\frac{\partial S}{\partial x_i}\right) + \underbrace{n_i \frac{\partial S}{\partial x_j}\frac{\partial u_j}{\partial x_i}}_{=-g_S a_S} \\ &= \underbrace{n_i n_i}_{=1} u_j \frac{\partial g_S}{\partial x_j} + u_j g_S \underbrace{n_i \frac{\partial n_i}{\partial x_j}}_{=0} - g_S a_S \\ &= \mathbf{u} \cdot \nabla g_S - g_S a_S, \end{aligned} \tag{A.3}$$

where $a_S = -\mathbf{n}_S \cdot \partial \mathbf{u}/\partial n_S$. Replacing in Eq. (A.2) and conveniently re-arranging we obtain

$$\frac{\partial g_S}{\partial t} = -\mathbf{u} \cdot \nabla g_S + g_S a_S + \frac{\partial \Gamma_S}{\partial n_S}, \tag{A.4}$$

which corresponds to the final form required in Section 2 (see Eq. (26)).

Appendix B. Detailed transformation of Γ_{Y_k} and Γ_T

In order to obtain the final form of the chemical species and temperature composition space equations, Eqs. (38) and (39), Γ_{Y_k} and Γ_T need to be transformed from physical into composition space. According to Eqs. (31) and (32), these terms are

$$\Gamma_{Y_k} = \frac{1}{\rho}\nabla \cdot (\rho D \nabla Y_k) + \frac{\dot{\omega}_k}{\rho} \tag{B.1}$$

and

$$\Gamma_T = \frac{1}{\rho}\nabla \cdot (\rho D \nabla T) + \frac{\dot{\omega}_T}{\rho} + \frac{D}{c_p}\nabla T \cdot \nabla c_p + \sum_{k=1}^{N} \frac{c_{p,k}}{c_p} D \nabla Y_k \cdot \nabla T, \tag{B.2}$$

respectively. It is noted now that there are two kind of terms that need to be transformed in these equations, namely $\nabla\left(\rho D \nabla \psi\right)$ and $(\nabla \psi_1 \cdot \nabla \psi_2)$. The first of them can be generically transformed as

$$\begin{aligned}\nabla\left(\rho D \nabla \psi\right) &= \nabla \cdot \left(\rho D \left(\frac{\partial \psi}{\partial Z}\nabla Z + \frac{\partial \psi}{\partial \varphi}\nabla \varphi\right)\right) \\ &= \frac{\partial \psi}{\partial Z}\nabla \cdot (\rho D \nabla Z) + \rho D |\nabla Z|^2 \frac{\partial^2 \psi}{\partial Z^2} + \frac{\partial \psi}{\partial \varphi}\nabla \cdot (\rho D \nabla \varphi) + \rho D |\nabla \varphi|^2 \frac{\partial^2 \psi}{\partial \varphi^2} \\ &= \rho D |\nabla Z|^2 \frac{\partial^2 \psi}{\partial Z^2} + \rho D |\nabla \varphi|^2 \frac{\partial^2 \psi}{\partial \varphi^2} + \Gamma_Z \frac{\partial \psi}{\partial Z} + \Gamma_\varphi \frac{\partial \psi}{\partial \varphi}. \end{aligned} \tag{B.3}$$

For the transformation of the second term, we make use of Eq. (11), which allows expressing the gradients of ψ_1 and ψ_2 as $\nabla \psi_1 = \partial \psi_1/\partial Z \; \nabla Z + \partial \psi_1/\partial \varphi \; \nabla \varphi$ and $\nabla \psi_2 = \partial \psi_2/\partial Z \; \nabla Z + \partial \psi_2/\partial \varphi \; \nabla \varphi$, respectively. After multiplying both expressions and properly arranging terms, we obtain

$$\nabla \psi_1 \cdot \nabla \psi_2 = |\nabla Z|^2 \frac{\partial \psi_1}{\partial Z}\frac{\partial \psi_2}{\partial Z} + |\nabla \varphi|^2 \frac{\partial \psi_1}{\partial \varphi}\frac{\partial \psi_2}{\partial \varphi} + \left(\frac{\partial \psi_1}{\partial Z}\frac{\partial \psi_2}{\partial \varphi} + \frac{\partial \psi_1}{\partial \varphi}\frac{\partial \psi_2}{\partial Z}\right)\underbrace{(\nabla Z \cdot \nabla \varphi)}_{=0}. \tag{B.4}$$

With Eqs. (B.3) and (B.4), Γ_{Y_k} and Γ_T can be rewritten in their final forms as

$$\Gamma_{Y_k} = \frac{1}{\rho}\left(\rho D g_Z^2 \frac{\partial^2 Y_k}{\partial Z^2} + \rho D g_\varphi^2 \frac{\partial^2 Y_k}{\partial \varphi^2} + \Gamma_Z \frac{\partial Y_k}{\partial Z} + \Gamma_\varphi \frac{\partial Y_k}{\partial \varphi}\right) + \frac{\dot{\omega}_k}{\rho} \tag{B.5}$$

and

$$\begin{aligned}\Gamma_T = &\frac{1}{\rho}\left(\rho D g_Z^2 \frac{\partial^2 T}{\partial Z^2} + \rho D g_\varphi^2 \frac{\partial^2 T}{\partial \varphi^2} + \Gamma_Z \frac{\partial T}{\partial Z} + \Gamma_\varphi \frac{\partial T}{\partial \varphi}\right) + \frac{\dot{\omega}_T}{\rho} \\ &+ \frac{D}{c_p}\left(|\nabla Z|^2 \frac{\partial T}{\partial Z}\frac{\partial c_p}{\partial Z} + |\nabla \varphi|^2 \frac{\partial T}{\partial \varphi}\frac{\partial c_p}{\partial \varphi}\right) \\ &+ \sum_{k=1}^{N} \frac{c_{p,k}}{c_p} D\left(|\nabla Z|^2 \frac{\partial Y_k}{\partial Z}\frac{\partial T}{\partial Z} + |\nabla \varphi|^2 \frac{\partial Y_k}{\partial \varphi}\frac{\partial T}{\partial \varphi}\right),\end{aligned} \tag{B.6}$$

respectively.

Appendix C. Consistency with Scholtissek et al. [22]

Scholtissek et al. [22] have recently derived a set of composition space equations in an orthogonal coordinate system built in terms of the mixture fraction and a reaction progress variable governed by Eqs. (33) and (34), respectively. The approach employs a Lagrangian particle traveling with a mixture fraction iso-surface, but which is free to move along them with the flow velocity. The required orthogonal space is then defined in terms of the transformation given by Eq. (1). Before further assumptions are introduced, their composition space equation for chemical species mass fractions yields [22]

$$\begin{aligned}\rho \frac{\partial Y_k}{\partial \tau} = &\rho D |\nabla Z|^2 \frac{\partial^2 Y_k}{\partial Z^2} + \rho D |\nabla_\perp Y_c|^2 \left.\frac{\partial^2 Y_k}{\partial Y_c^2}\right|_Z \\ &+ \left.\frac{\partial Y_c}{\partial \tau}\frac{\partial Y_k}{\partial Y_c}\right|_Z - \dot{\omega}_{c_\perp}\left.\frac{\partial Y_k}{\partial Y_c}\right|_Z + \dot{\omega}_k,\end{aligned} \tag{C.1}$$

with

$$\dot{\omega}_{c_\perp} = \rho D |\nabla Z|^2 \frac{\partial^2 Y_c}{\partial Z^2} + \dot{\omega}_c. \tag{C.2}$$

While the same procedure was used in that work for the derivation of a composition space equation for the temperature, we will focus here on Eq. (C.1) only, since it already contains all the necessary terms to evaluate conditions for equivalence between their equations and the ones introduced in the present work.

We proceed now to analyze conditions required to achieve equivalence between Eqs. (38) and (C.1). For this, we note first that the condition $\nabla \varphi = \nabla_\perp Y_c$ directly implies that

$$\frac{\partial Y_k}{\partial \varphi} = \left.\frac{\partial Y_k}{\partial Y_c}\right|_Z \quad \text{and} \quad \frac{\partial^2 Y_k}{\partial \varphi^2} = \left.\frac{\partial^2 Y_k}{\partial Y_c^2}\right|_Z, \tag{C.3}$$

and that the chemical source term appearing in Eq. (38) is identical to the one given by Eq. (C.3). However, despite these similarities, some important differences still remain. First, the temporal derivative of Y_k (with respect to τ) is different for both approaches. In particular, in the formulation presented in the current work this quantity is computed considering a particle moving with two scalar isosurfaces. In contrast, as stated above, Scholtissek et al. [22] allow the particle to move with the flow field in the direction tangential to ∇Z. A further difference observed is the term $\rho \frac{\partial Y_c}{\partial \tau} \frac{\partial Y_k}{\partial Y_c}$ appearing in Eq. (C.1), which does not have a counterpart in Eq. (38). The equivalence between the different transient terms can be better understood by considering the change of variable $(Z, \varphi, \tau) \rightarrow (Z, Y_c(Z, \varphi, \tau), \tau)$, which, after applying the chain rule, allows rewriting the transient term in Eq. (38) in the following equivalent way

$$\left.\frac{\partial Y_k}{\partial \tau}\right|_{Z,\varphi} = \left.\frac{\partial Y_k}{\partial \tau}\right|_{Z,Y_c} + \left.\frac{\partial Y_c}{\partial \tau}\right|_{Z,\varphi} \left.\frac{\partial Y_k}{\partial Y_c}\right|_{Z,\tau} . \tag{C.4}$$

Thus, with this it becomes clear that the differences regarding the transient terms are apparent only. Despite the exact relation existing between them, having a single transient term evidently results in an easier to handle formulation.

Appendix D. The transformation $(Z, \varphi) \rightarrow (Z^*, \varphi^*)$

The 2D composition space equations are formulated in (Z,φ)-space, but they are solved in the normalized (Z^*, φ^*)-space, cf. Fig. 2. In this section, we describe how the change in variables leads to a reformulation of the terms appearing in the equations. With this, the composition space equations can be evaluated on a (Z^*, φ^*)-grid to facilitate their numerical solution.

The transformation rules for the change of variables $(Z, \varphi) \rightarrow (Z^*, \varphi^*)$ are repeated here for the readers convenience:

$$Z^*(Z) = \frac{Z - Z_{\min}}{Z_{\max} - Z_{\min}} , \tag{D.1}$$

$$\varphi^*(\varphi, Z) = \frac{\varphi - \varphi_{\min}}{\varphi_{\max}(Z) - \varphi_{\min}} . \tag{D.2}$$

For consistency, we further introduce the time-like coordinate τ^* with the trivial transformation $\tau^* = \tau$. In the above transformation, the quantities $\varphi_{\min}$ and $\varphi_{\max}$ correspond to the values of the progress variable at the lower and upper boundary, respectively. For the current case, the progress variable is defined as $Y_c = Y_{\mathrm{H_2O}} + Y_{\mathrm{CO_2}}$. Thus, $\varphi_{\min} = 0$ (fresh gas conditions at lower boundary) and $\varphi_{\max}(Z) = Y_c(Z)$ is a case-specific function of mixture fraction to be determined from the non-premixed flamelet solution prescribed for the upper boundary. For the normalization of mixture fraction, $Z_{\min} = 0.0284$ ($\phi = 0.5$) and $Z_{\min} = 0.0903$ ($\phi = 1.7$) which are both constants independent from Z or φ.

For the change of variables, it is useful to formulate the jacobian:

$$\frac{\partial(\tau^*, Z^*, \varphi^*)}{\partial(\tau, Z, \varphi)} = \begin{bmatrix} \frac{\partial \tau^*}{\partial \tau} & \frac{\partial \tau^*}{\partial Z} & \frac{\partial \tau^*}{\partial \varphi} \\ \frac{\partial Z^*}{\partial \tau} & \frac{\partial Z^*}{\partial Z} & \frac{\partial Z^*}{\partial \varphi} \\ \frac{\partial \varphi^*}{\partial \tau} & \frac{\partial \varphi^*}{\partial Z} & \frac{\partial \varphi^*}{\partial \varphi} \end{bmatrix} = \begin{bmatrix} 1 & 0 & 0 \\ 0 & \frac{1}{\Delta Z} & 0 \\ 0 & -\frac{\varphi^*}{\Delta \varphi}\frac{\partial \varphi_{\max}}{\partial Z} & \frac{1}{\Delta \varphi} \end{bmatrix}. \tag{D.3}$$

Utilizing these transformation rules, the partial derivatives with respect to τ, Z, and φ can be rewritten as

$$\frac{\partial(\cdot)}{\partial \tau} = \frac{\partial \tau^*}{\partial \tau}\frac{\partial T}{\partial \tau^*} + \frac{\partial Z^*}{\partial \tau}\frac{\partial T}{\partial Z^*} + \frac{\partial \varphi^*}{\partial \tau}\frac{\partial T}{\partial \varphi^*} = \frac{\partial T}{\partial \tau^*}, \tag{D.4}$$

$$\frac{\partial T}{\partial Z} = \frac{\partial \tau^*}{\partial Z}\frac{\partial T}{\partial \tau^*} + \frac{\partial Z^*}{\partial Z}\frac{\partial T}{\partial Z^*} + \frac{\partial \varphi^*}{\partial Z}\frac{\partial T}{\partial \varphi^*} = \frac{1}{\Delta Z}\frac{\partial T}{\partial Z^*} - \frac{\varphi^*}{\Delta \varphi}\frac{\partial \varphi_{\max}}{\partial Z}\frac{\partial T}{\partial \varphi^*}, \tag{D.5}$$

and

$$\frac{\partial T}{\partial \varphi} = \frac{\partial \tau^*}{\partial \varphi}\frac{\partial T}{\partial \tau^*} + \frac{\partial Z^*}{\partial \varphi}\frac{\partial T}{\partial Z^*} + \frac{\partial \varphi^*}{\partial \varphi}\frac{\partial T}{\partial \varphi^*} = \frac{1}{\Delta \varphi}\frac{\partial T}{\partial \varphi^*}. \tag{D.6}$$

Applying the above math to the second partial derivatives with respect to Z and φ, one obtains the transformation rules provided in Eqs. 50 and 51.

Appendix E. Transformed composition space equations

The composition space equations for species and temperature in (Z^*, φ^*)-space read

$$\rho\frac{\partial Y_k}{\partial \tau^*} + \frac{\dot{\omega}_\varphi}{\Delta \varphi}\frac{\partial Y_k}{\partial \varphi^*} = \frac{\rho D g_Z^2}{\Delta Z^2}\frac{\partial^2 Y_k}{\partial {Z^*}^2} + \frac{\rho D g_\varphi^2}{\Delta \varphi^2}\frac{\partial^2 Y_k}{\partial {\varphi^*}^2} + \rho D g_Z^2\left[m_1\frac{\partial^2 Y_k}{\partial \varphi^* \partial Z^*} + m_2\frac{\partial^2 Y_k}{\partial {\varphi^*}^2} + m_3\frac{\partial Y_k}{\partial \varphi^*}\right] + \dot{\omega}_k \tag{E.1}$$

and

$$\rho\frac{\partial T}{\partial \tau^*}+\frac{\dot{\omega}_\varphi}{\Delta\varphi}\frac{\partial T}{\partial \varphi^*}=\frac{\rho D g_Z^2}{\Delta Z^2}\frac{\partial^2 T}{\partial Z^{*2}}+\frac{\rho D g_\varphi^2}{\Delta\varphi^2}\frac{\partial^2 T}{\partial \varphi^{*2}}$$
$$+\frac{\rho D}{c_p}\left[g_Z^2\left(\frac{1}{\Delta Z}\frac{\partial T}{\partial Z^*}+m_0\frac{\partial T}{\partial \varphi^*}\right)\left(\frac{1}{\Delta Z}\frac{\partial c_p}{\partial Z^*}+m_0\frac{\partial c_p}{\partial \varphi^*}\right)+\frac{g_\varphi^2}{\Delta\varphi^2}\frac{\partial T}{\partial \varphi^*}\frac{\partial c_p}{\partial \varphi^*}\right]$$
$$+\sum_{k=1}^{N}\frac{c_{p,k}}{c_p}\left[\rho D g_Z^2\left(\frac{1}{\Delta Z}\frac{\partial Y_k}{\partial Z^*}+m_0\frac{\partial Y_k}{\partial \varphi^*}\right)\left(\frac{1}{\Delta Z}\frac{\partial T}{\partial Z^*}+m_0\frac{\partial T}{\partial \varphi^*}\right)+\frac{\rho D g_\varphi^2}{\Delta\varphi^2}\frac{\partial Y_k}{\partial \varphi^*}\frac{\partial T}{\partial \varphi^*}\right]$$
$$+\rho D g_Z^2\left[m_1\frac{\partial^2 T}{\partial \varphi^*\partial Z^*}+m_2\frac{\partial^2 T}{\partial \varphi^{*2}}+m_3\frac{\partial T}{\partial \varphi^*}\right]+\dot{\omega}_T\,, \tag{E.2}$$

respectively. Additionally, the corresponding equations for g_Z and g_φ are

$$\frac{\partial g_Z}{\partial \tau^*}=-\left[\frac{g_\varphi}{\rho\Delta\varphi}\frac{\partial}{\partial \varphi^*}\left(\rho D g_\varphi\right)-D g_\varphi\kappa_\varphi+\frac{\dot{\omega}_\varphi}{\rho}\right]\frac{1}{\Delta\varphi}\frac{\partial g_Z}{\partial \varphi^*}$$
$$+\frac{g_Z^2}{\rho\Delta Z^2}\frac{\partial^2}{\partial Z^{*2}}\left(\rho D g_Z\right)-g_Z^2\left(\frac{1}{\Delta Z}\frac{\partial}{\partial Z^*}\left(D\kappa_Z\right)+m_0\frac{\partial}{\partial \varphi^*}\left(D\kappa_Z\right)\right)$$
$$-\frac{g_Z^2}{\rho^2}\left(\frac{1}{\Delta Z}\frac{\partial \rho}{\partial Z^*}+m_0\frac{\partial \rho}{\partial \varphi^*}\right)\left(\frac{1}{\Delta Z}\frac{\partial}{\partial Z^*}\left(\rho D g_Z\right)+m_0\frac{\partial}{\partial \varphi^*}\left(\rho D g_Z\right)\right)$$
$$+\frac{g_Z^2}{\rho}\left[m_1\frac{\partial^2}{\partial \varphi^*\partial Z^*}\left(\rho D g_Z\right)+m_2\frac{\partial^2}{\partial \varphi^{*2}}\left(\rho D g_Z\right)+m_3\frac{\partial}{\partial \varphi^*}\left(\rho D g_Z\right)\right]+g_Z a_Z \tag{E.3}$$

and

$$\frac{\partial g_\varphi}{\partial \tau^*}=-\left[\frac{g_Z}{\rho}\left(\frac{1}{\Delta Z}\frac{\partial}{\partial Z^*}\left(\rho D g_Z\right)+m_0\frac{\partial}{\partial \varphi^*}\left(\rho D g_Z\right)\right)-D g_Z\kappa_Z\right]\left(\frac{1}{\Delta Z}\frac{\partial g_\varphi}{\partial Z^*}+m_0\frac{\partial g_\varphi}{\partial \varphi^*}\right)$$
$$+\frac{g_\varphi^2}{\rho\Delta\varphi^2}\frac{\partial^2}{\partial \varphi^{*2}}\left(\rho D g_\varphi\right)-\frac{g_\varphi^2}{\rho^2\Delta\varphi^2}\frac{\partial \rho}{\partial \varphi^*}\frac{\partial}{\partial \varphi^*}\left(\rho D g_\varphi\right)$$
$$-\frac{g_\varphi^2}{\Delta\varphi}\frac{\partial\left(D\kappa_\varphi\right)}{\partial \varphi^*}+\frac{g_\varphi^2}{\Delta\varphi}\frac{\partial}{\partial \varphi^*}\left(\frac{\dot{\omega}_\varphi}{\rho g_\varphi}\right)+g_\varphi a_\varphi\,, \tag{E.4}$$

where m_0 - m_3 represent metric terms defined as

$$m_0=-\frac{\varphi^*}{\Delta\varphi}\frac{\partial \varphi_{\max}}{\partial Z},$$
$$m_1=-2\frac{\varphi^*}{\Delta\varphi\Delta Z}\frac{\partial \varphi_{\max}}{\partial Z},$$
$$m_2=\frac{\varphi^{*2}}{(\Delta\varphi)^2}\left(\frac{\partial \varphi_{\max}}{\partial Z}\right)^2,$$

and

$$m_3=\frac{2\varphi^*}{(\Delta\varphi)^2}\left(\frac{\partial \varphi_{\max}}{\partial Z}\right)^2-\frac{\varphi^*}{\Delta\varphi}\frac{\partial^2 \varphi_{\max}}{\partial Z^2}.$$

References

[1] N. Peters, Laminar diffusion flamelet models in non-premixed turbulent combustion, Prog. Energy Combust. Sci. 10 (1984) 319 – 339.

[2] H. Pitsch, N. Peters, A consistent flamelet formulation for non-premixed combustion considering differential diffusion effects, Combust. Flame 114 (1998) 26 – 40.

[3] A. Scholtissek, W. L. Chan, H. Xu, F. Hunger, H. Kolla, J. H. Chen, M. Ihme, C. Hasse, A multi-scale asymptotic scaling and regime analysis of flamelet equations including tangential diffusion effects for laminar and turbulent flames, Combust. Flame 162 (2015) 1507 – 1529.

[4] A. Scholtissek, F. Dietzsch, M. Gauding, C. Hasse, In-situ tracking of mixture fraction gradient trajectories and unsteady flamelet analysis in turbulent non-premixed combustion, Combust. Flame 175 (2017) 243 – 258.

[5] J. A. van Oijen, L. P. H. de Goey, Modelling of premixed laminar flames using flamelet-generated manifolds, Combust. Sci. Technol. 161 (2000) 113–137.

[6] J. A. van Oijen, F. A. Lammers, L. P. H. de Goey, Modeling of complex premixed burner systems by using flamelet-generated manifolds, Combust. Flame 127 (2001) 2124 – 2134.

[7] J. A. van Oijen, A. Donini, R. J. M. Bastiaans, J. H. M. ten Thije Boonkkamp, L. P. H. de Goey, State-of-the-art in premixed combustion modeling using flamelet generated manifolds, Prog. Energy Combust. Sci. 57 (2016) 30–74.

[8] A. Scholtissek, P. Domingo, L. Vervisch, C. Hasse, A self-contained progress variable space solution method for thermochemical variables and flame speed in freely-propagating premixed flamelets, Proc. Combust. Inst. 37 (2018) 1529 – 1536.

[9] A. Scholtissek, P. Domingo, L. Vervisch, C. Hasse, A self-contained composition space solution method for strained and curved premixed flamelets, Combust. Flame 207 (2019) 342–355.

[10] K. Luo, J. Fan, K. Cen, New spray flamelet equations considering evaporation effects in the mixture fraction space, Fuel 103 (2013) 1154 – 1157.

[11] H. Olguin, E. Gutheil, Influence of evaporation on spray flamelet structures, Combust. Flame 161 (2014) 987 – 996.

[12] H. Olguin, E. Gutheil, Theoretical and numerical study of evaporation effects in spray flamelet modeling, in: B. Merci, E. Gutheil (Eds.), Experiments and Numerical Simulations of Turbulent Combustion of Diluted Sprays, Vol. 19 of ERCOFTAC Series, Springer International Publishing, 2014, pp. 79–106.

[13] H. Olguin, E. Gutheil, Derivation and evaluation of a multi-regime spray flamelet model, Zeitschrift für Physikalische Chemie (2014) 461–482.

[14] H. Olguin, A. Scholtissek, S. Gonzalez, F. Gonzalez, M. Ihme, C. Hasse, E. Gutheil, Closure of the scalar dissipation rate in the spray flamelet equations through a transport equation for the gradient of the mixture fraction, Combust. Flame 208 (2019) 330–350.

[15] N. Peters, Turbulent Combustion, Cambridge University Press, 2000.

[16] A. Masri, Partial premixing and stratification in turbulent flames, Proc. Combust. Inst. 35 (2015) 1115 – 1136.

[17] P. Domingo, L. Vervisch, D. Veynante, Large-Eddy Simulation of a lifted methane jet flame in a vitiated coflow, Combust. Flame 152 (2008) 415 – 432.

[18] E. Knudsen, H. Pitsch, A general flamelet transformation useful for distinguishing between premixed and non-premixed modes of combustion, Combust. Flame 156 (2009) 678 – 696.

[19] P.-D. Nguyen, L. Vervisch, V. Subramanian, P. Domingo, Multidimensional flamelet-generated manifolds for partially premixed combustion, Combust. Flame 157 (2010) 43 – 61.

[20] E. Knudsen, H. Pitsch, Capabilities and limitations of multi-regime flamelet combustion models, Combust. Flame 159 (2012) 242 – 264.

[21] M. E. Mueller, Physically-derived reduced-order manifold-based modeling for multi-modal turbulent combustion, Combust. Flame 214 (2020) 287 – 305.

[22] A. Scholtissek, S. Popp, S. Hartl, H. Olguin, P. Domingo, L. Vervisch, C. Hasse, Derivation and analysis of two-dimensional composition space equations for multi-regime combustion using orthogonal coordinates, Combust. Flame 218 (2020) 205 – 217.

[23] A. G. Novoselov, B. A. Perry, M. E. Mueller, Two-dimensional manifold equations for multi-modal turbulent combustion: Nonpremixed combustion limit and scalar dissipation rates, Combust. Flame 231 (2021) 111475.

[24] C. Hasse, N. Peters, A two mixture fraction flamelet model applied to split injections in a DI diesel engine, Proc. Combust. Inst. 30 (2005) 2755 – 2762.

[25] V. Mittal, D. J. Cook, H. Pitsch, An extended multi-regime flamelet model for IC engines, Combust. Flame 159 (2012) 2767 – 2776.

[26] G. Lodier, L. Vervisch, V. Moureau, P. Domingo, Composition-space premixed flamelet solution with differential diffusion for in situ flamelet-generated manifolds, Combust. Flame 158 (2011) 2009 – 2016.

[27] C. H. Gibson, Fine structure of scalar fields mixed by turbulence. i. zero gradient points and minimal gradient surfaces, Phys. Fluids 11 (1968) 2305–2315.

[28] A. Y. Klimenko, On the relation between the conditional moment closure and unsteady flamelets, Combust. Theory Model. 5 (2001) 275–294.

[29] H. Olguin, F. Huenchuguala, Z. Sun, C. Hasse, A. Scholtissek, Three questions regarding scalar gradient equations in flamelet theory, Combust. Flame 249 (2023) 112624.

[30] L. P. H. de Goey, J. H. M. ten Thije Boonkkamp, A mass-based definition of flame stretch for flames with finite thickness, Combust. Sci. Technol. 122 (1997) 399–405.

[31] L. P. H. de Goey, J. H. M. ten Thije Boonkkamp, A flamelet description of premixed laminar flames and the relation with flame stretch, Combust. Flame 119 (1999) 253–271.

[32] B. Fiorina, O. Gicquel, L. Vervisch, S. Carpentier, N. Darabiha, Approximating the chemical structure of partially premixed and diffusion counterflow flames using fpi flamelet tabulation, Combust. Flame 140 (2005) 147 – 160.

[33] J. Douglas, J. E. Gunn, A general formulation of alternating direction methods: Part I. Parabolic and hyperbolic problems, Numerische Mathematik 6 (1964) 428–453.

[34] D. G. Goodwin, H. K. Moffat, I. Schoegl, R. L. Speth, B. W. Weber, Cantera: An object-oriented software toolkit for chemical kinetics, thermodynamics, and transport processes, `https://www.cantera.org`, version 2.6.0 (2022).

[35] G. P. Smith, D. M. Golden, M. Frenklach, N. W. Moriarty, B. Eiteneer, M. Goldenberg, C. T. Bowman, R. K. Hanson, S. Song, W. C. G. Jr., V. V. Lissianski, Z. Qin, Gri-mech 3.0, `http://www.me.berkeley.edu/gri_mech/` (1999).

[36] C. Olbricht, O. T. Stein, J. Janicka, J. van Oijen, S. Wysocki, A. M. Kempf, LES of lifted flames in a gas turbine model combustor using top-hat filtered PFGM chemistry, Fuel 96 (2012) 100–107.

[37] F. Proch, A. M. Kempf, Numerical analysis of the Cambridge stratified flame series using artificial thickened flame LES with tabulated premixed flame chemistry, Combust. Flame 161 (2014) 2627–2646.

[38] J.-B. Michel, O. Colin, D. Veynante, Modeling ignition and chemical structure of partially premixed turbulent flames using tabulated chemistry, Combust. Flame 152 (2008) 80–99.

[39] S. Popp, S. Hartl, D. Butz, D. Geyer, A. Dreizler, L. Vervisch, C. Hasse, Assessing multi-regime combustion in a novel burner configuration with large eddy simulations using tabulated chemistry, Proc. Combust. Inst. 38 (2021) 2551–2558.

[40] S. Richard, O. Colin, O. Vermorel, A. Benkenida, C. Angelberger, D. Veynante, Towards large eddy simulation of combustion in spark ignition engines, Proc. Combust. Inst. 31 (2007) 3059–3066.

[41] C. Dopazo, J. Martín, Local geometry of isoscalar surfaces, Phys. Rev. E 76 (2007) 056326.